Journal of Science Research and Reviews

PRINT ISSN: 1595-9074
E-ISSN: 1595-8329
DOI: https://doi.org/10.70882/josrar.2025.v2i3.79
Homepage: https://josrar.esrgngr.org

Original Research Article

Comparative Analysis Between 2D-Electrical Imaging and Seismic Refraction Tomography at National Animal Production Research Institute (NAPRI), Zaria. Kaduna State, Nigeria

***[1]Adamu, John, [1]Usman, Aliyu, [2]Bello, Ezekiel and [2]Issa, Mohammed**

[1]Department of Physical Sciences, Niger State Polytechnic, Zungeru, Nigeria
[2]Department of Electrical Engineering, Niger State Polytechnic, Zungeru, Nigeria
*Corresponding Author's email: get2johnny2013@gmail.com

KEYWORDS

Geoelectric imaging,
Pseudosections,
Refraction Seismic Tomography,
Seismic Tomography models.

ABSTRACT

Understanding subsurface structure is crucial in geotechnical, environmental and engineering investigations. Two widely used geophysical methods are: 2D Electrical Resistivity Tomography (ERT) and Seismic Refraction Tomography (SRT). They offer complementary insights into subsurface conditions. ERT is sensitive to electrical properties (e.g. moisture, clay content), while SRT excels in detecting mechanical contrasts (e.g. rock hardness), combing both methods enhances subsurface imaging accuracy, especially in complex geology like fault zero or weathered profiles. The two methods were carried out to investigate the depth to basement complex in National Animal Production Research Institute (NAPRI), Zaria. The major instruments used for this survey where Terraloc Mark6 digital seismography, sets of vertical geophones, SAS4000 Terrameter and Electrode Selector ES 464. The geometric arrangement positioned both the geophones and the source along a straight line. The 24 geophones and the source were set at 5 m intervals, covering a distance of 120 m. Besides the initial shot location, shots were detonated at each geophone location. For the 2D electrical survey, the electrodes were arranged along the profiles with a 5.0 m electrode spacing between the 41 electrodes, resulting in a total spread of 200 m. In each of the profiles, geo-electric tomography managed to penetrate to a maximum depth of 29.3 m with optimal current injection into the subsurface. The geo-electric tomography was unable to reach the basement rock except at locations where the basement complex is found at a depth of 29.3 m or less. In contrast, seismic refraction tomography achieved a penetration depth of over 40m. It was possible to identify the basement tomography at depths exceeding 40m along the profiles.

CITATION

Adamu, J., Usman, A., Bello, E., & Issa, M. (2025). Comparative Analysis Between 2D-Electrical Imaging and Seismic Refraction Tomography at National Animal Production Research Institute (NAPRI), Zaria. Kaduna State, Nigeria. *Journal of Science Research and Reviews*, *2*(3), 59-65. https://doi.org/10.70882/josrar.2025.v2i3.79

INTRODUCTION

Tomography is a general imaging technique used to examine internal structures of objects ranging from human anatomy to geological formations by reconstructing cross-sectional images from transmitted signals (Alan & Aftab, 2000). In geophysics, tomography encompasses methods such as electrical resistivity tomography (ERT) and seismic refraction tomography (SRT), which are widely applied in subsurface investigations. ERT utilizes arrays of electrodes to measure voltage differences resulting from injected currents, enabling the estimation of subsurface resistivity distributions. These resistivity values are influenced by geological parameters such as porosity, water saturation, and mineral composition (Loke, 2000).

Seismic refraction tomography, on the other hand, interprets the travel times of seismic waves to model subsurface velocity structures. It is particularly effective in environments where seismic velocity increases with depth, allowing for detailed imaging of weathered layers, water tables, and bedrock interfaces (Lowrie, 1997; Gregory, 2002)

Recent studies have demonstrated that SRT can outperform ERT in terms of depth penetration, especially in urban or constrained settings where spread length is limited.

The integration of both methods ERT and SRT has proven valuable in delineating basement topography and characterizing subsurface heterogeneity. For instance, Aka et al. (2020) showed that combining these techniques enhances the detection of landslide-prone zones and improves geotechnical assessments. Therefore, the current study aims to compare the maximum depth of penetration achievable by seismic refraction tomography relative to geo-electric tomography under similar spread constraints, and to define the basement topography along a shared profile.

MATERIALS AND METHODS

Location of the Survey Area

Shika in Zaria is situated within the northern Nigerian Basement Complex, (Fig. 1). It lies between latitudes 11^{0}12'4.6"N and 11^{0}12'10.2"N and longitudes 7^{0}33'50.2"E and 7^{0}33'64.5"E within the Zaria sheet 102. The mean elevation of the area is about 700m above mean sea level. Figure 1.2 is the National Animal Production Research Institute (NAPRI), location map showing the investigated site. The study area (NAPRI) is located inside Shika, where the profiles are laid, is bounded by latitude 11^{0}12'16.1"N to latitude 11^{0}12'23.8"N and longitude 7^{0}33'37.6"E to longitude 7^{0}33'48.6"E, with an average elevation of 683m above sea level.

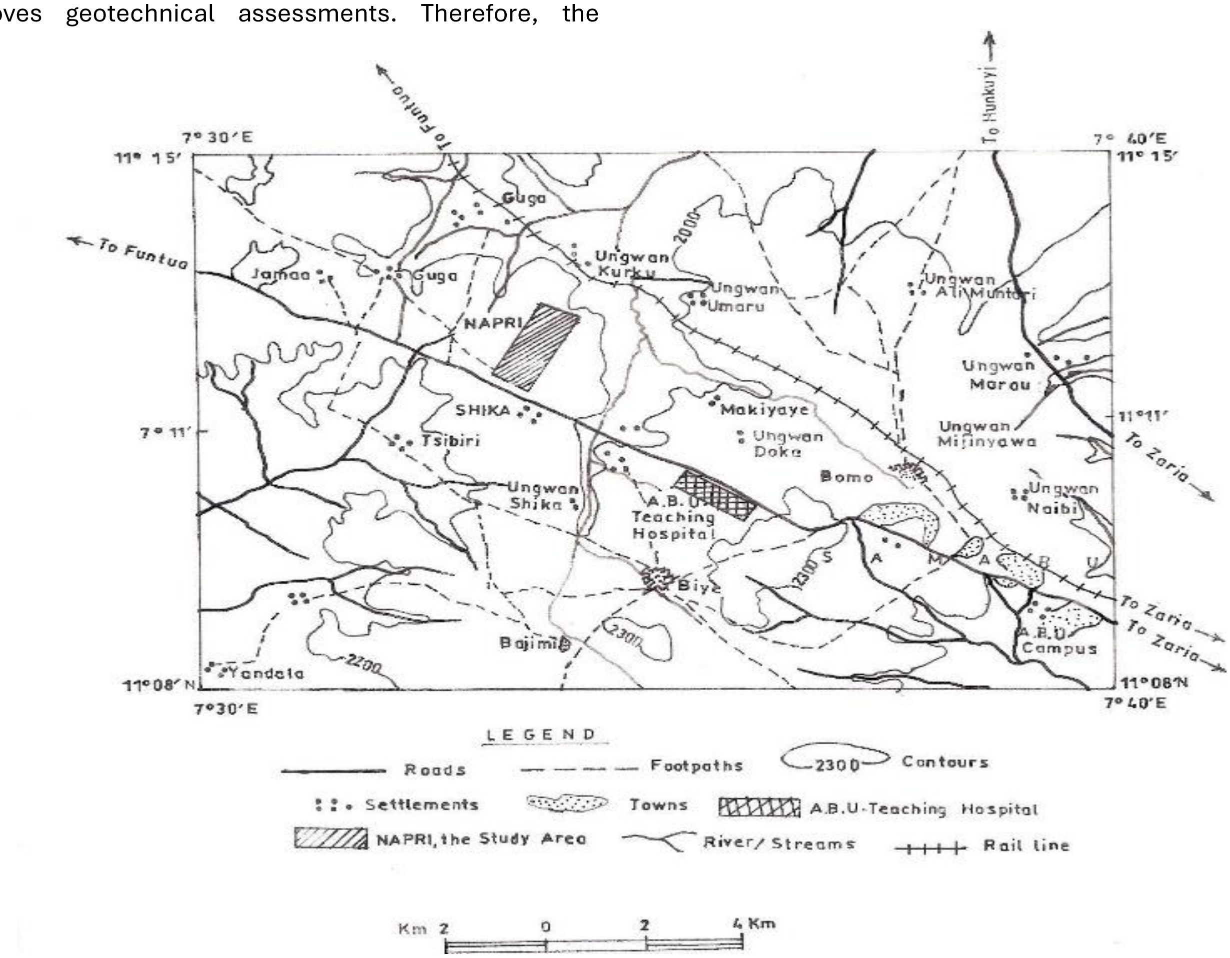

Figure 1: Location Map showing the Study Area (Part of Zaria Sheet 102)

Geology of the Study Area

Nigeria lies in the Pan-African mobile belt which has been affected by Pan-African events through the ages of orogenic, epeirogenetic, tectonic and metamorphic cycles.

The study area is part of the Nigerian Basement Complex underlain by crystalline rocks, so the geology of the area is the same as that of the Nigerian Basement complex. The rocks of the Basement Complex occupy more than 50% of the total land surface of Nigeria, and accommodate the metasediments which are made up of gneisses. Exposures are scanty and highly weathered. The rock types are biotites, gneisses, granite gneisses and in parts with subordinate migmatites. The contact between the gneisses and metasediments are gradational (McCurry, 1970). Shika in Zaria is underlain by basement complex rocks (Fig. 2) of Precambrian age. The rocks are mainly granites, gneisses, and schists. Oyewoye (1964) has shown that there is a structural relationship between this Basement Complex and the rest of the West African basement. This is partly due to the fact that the whole region was involved in a single set of orogenic episode, the Pan African orogeny, which left an imprint of structural similarity upon the rock units.

Granitic intrusions form a suite of batholiths (the Zaria Batholiths), part of which outcrops as the Kufena Hill. The gneisses are found as small belts within the granite intrusions, and are also found east and west of the batholiths. The biotite gneiss extends westwards to form a gradational boundary with the schist belt. The gneiss continues eastwards to some extent and is occasionally broken up by the Older Granite (McCurry, 1970). The Older Granite intrusion is supposed to have been formed at the bottom of a fold mountain belt (Wright and McCurry, 1970).

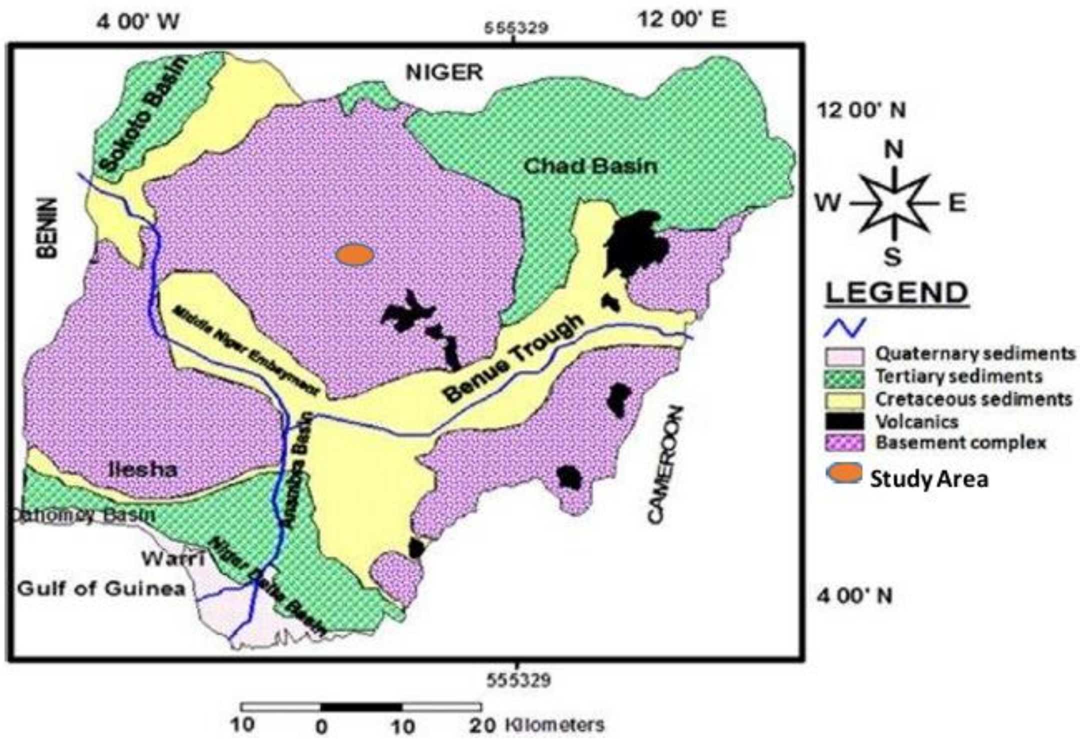

Figure 2: Geological Map of Nigeria showing Basement Complex and Sedimentary terrain (Ologe et. al., 2014)

Material

For Resistivity Method

The ABEM Lund imaging system was used for the data acquisition. It consists of:

1. ABEM Terrameter SAS4000;
2. ABEM Electrode Selector ES464, including connectors to Terrameter (serial port and current/voltage terminals);
3. ABEM SAS External Battery Adaptor (EBA) Reels of Cables and
4. Electrodes and Jumpers.

For Seismic Method

A 24 channel Terraloc Mk6(seismograph), vertical geophones, two reels of cables, a sledge hammer for energy source, a base plate, a measuring tape, a rechargeable cell, a chisel, two raging poles were used for this research . This is because the basic technique of the seismic exploration consists of generating seismic waves and measuring the time required for the waves to travel from the source to a series of geophones, usually placed at certain intervals along a straight line directed towards the source (Telford et al., 1978). From the knowledge of travel times to the various geophones and the velocity of the waves, one can attempt to reconstruct the paths of the seismic waves.

Field Procedure

The field procedure employed for the geo-electric imaging included laying out the 42 steel electrodes along the profile which was connected to the multicore cable at 5m regular take-out intervals via sets of jumpers. This was adopted for the purposes of 5m electrode spacing in most of the profile. The measurement of apparent resistivity of the subsurface was carried out by the electrode selector ES 464 and the SAS 4000 Terrameter, where it was stored for onward processing. The seismic refraction method was conducted by planting the geophones at regular intervals of 5m along the profile. An initial offset distance of 15m was used, shots were fired at a regular interval distance of 5m before the first geophone at each geophone point, in between the geophones and beyond. The generated seismic refracted wave and its resultant seismogram were recorded by the seismograph where it was stored for further processing.

Data Processing and Theory

The processing of the measured geo-electric data was done using 2-dimensional resistivity (RES2DIV) imaging interpretation software. This interpretation software essentially calculates the true resistivity and true depth of the ground from the input data (apparent resistivity) file using a Jacobian matrix calculation with forward modeling procedures and robust least squares inversion algorithm with smoothing constraints. The results of the interpretation are displayed as a 2D electrical resistivity image of the subsurface along the line of the traverse. Calculated pseudosections were produced as replicas of the observed, and the corresponding true resistivity model was generated.

Spectrum analysis was carried out on the raw seismic data to determine the dominant frequency which constitutes the important seismic signal. A bandpass frequency was set to eliminate the seismic noise which could have marred the real seismic signals. The gain filter was applied to enhance the amplitude of the far trace. The first arrival times was then picked and used for inversion to generate a tomographic model, using the waveform inversion method.

The various theories of the two methods are outlined below.

The resistivity measurements are normally made by injecting current into the ground through two current electrodes (C1 and C2 in Figure 3), and measuring the resulting voltage difference at two potential electrodes (P1 and P2). From the current (I) and voltage (V) values, an apparent resistivity (ρ_a) value is calculated.

$$\rho_a = \frac{kV}{I} \qquad (1)$$

Where k is the geometric factor which depends on the arrangement of the four electrodes.

Resistivity meters normally give a resistance value, R=V/I, so in practice the apparent resistivity value is calculated by

$$\rho_a = kR \qquad (2)$$

The calculated resistivity value is not the true resistivity of the subsurface, but an “apparent” value which is the resistivity of a homogeneous ground which will give the same resistance value for the same electrode arrangement. The relationship between the “apparent” resistivity and the “true” resistivity is a complex relationship. To determine the true subsurface resistivity, an inversion of the measured apparent resistivity values using a computer program must be carried out (Loke, 2000).

The series expansion method which includes curved ray paths was used in the model computation of the seismic refraction tomography model. Thus for a given source receiver pair the line integral of the model function M(r) over the raypath is

$$P_{obs} = \int ray M^{true}(r)dr \qquad (3)$$

where the observed projection given by the data function P_{obs} represents the measured line integral (observed tomography data) and $M^{true}(r)$is the true model function which remains to be determined. The last equation is used to formulate the forward modeling by setting

$$P = \int ray M(r)dr \qquad (4)$$

Where P is now the predicted function and *M(r)* is the estimated model function. Thus forward modeling is defined as determining the predicted data function from the line integral along the raypath through known, but estimated, model function.

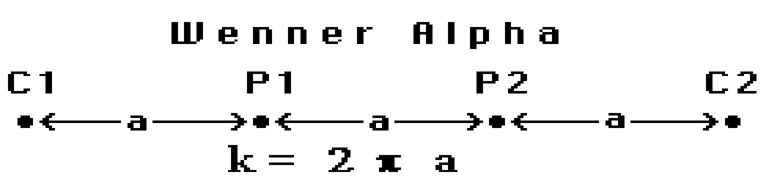

Figure 3: Wenner array with its geometric factor

For a discretized model function equation (4) is rewritten in discrete form, to describe ray through the discrete model function as

$$P = \sum_{i=1}^{f} M_i S_i \quad (5)$$

Where M_i is the estimated model function for the ith cell, S_i is the ray path length of the ray within the ith cell, and i is the total number of the cells in the gridded target.

The addition of extra rays will make all the cells to be interrogated by this network of rays. Therefore we modify the index of equation (4) to include a projection value for every ray. If P_i represents the projection, or line integral predicted for the i^{th} ray, then equation (4) is rewritten as

$$P = \sum_i^f M_i S_{ni} \text{ for } n = 1,2,3,\ldots. I \quad (6)$$

Where *I* is the total number of rays, S_{ni} is the path length of the n^{th} ray through the i^{th} cell (Tien-When, 2002).

RESULTS AND DISCUSSION

The inverse models for electrical resistivity and seismic tomography data along profile 1 are shown in Fig. 4. The electrical resistivity model has a spread length of 200 m and 3640 data points. The measured apparent resistivity data correlate very well with the calculated apparent resistivity data as can be seen in the two pseudosections presented in Fig. 4, therefore the model of the true resistivity can be accepted.

However, a comparison of their depth section indicated that the geoelectric section probed down to a depth of 29.3 m, while the seismic section indicated a depth of penetration of beyond 40 m.

The velocity values of the seismic tomography above 2000 m/s indicated that it probed up to the basement, unlike the resistivity section which indicated very low resistivity for two reasons. First, because the area is waterlogged, it tends to have a very high conductivity, and secondly, because the resistivity model did not get to the basement as a result of spread length limitation.

The inverse models for electrical resistivity and seismic tomography for profile 2 are shown in (Fig. 5).

The model section of the electrical resistivity method indicated that the current penetrated to a depth of 29.3 m, thereby giving rise to low resistivity values which are slightly higher than the values of profile 1. This is not unconnected to the limitation in spread length, which prevented the ejected optimum current from getting to the basement.

However, seismic tomography of the same spread length and taken along the same profile was able to probe up to a depth of 40 m, with very high resolution. The range of velocity indicated in the velocity colour bar for the model, is a clear indication that the seismic energy probed to be basement.

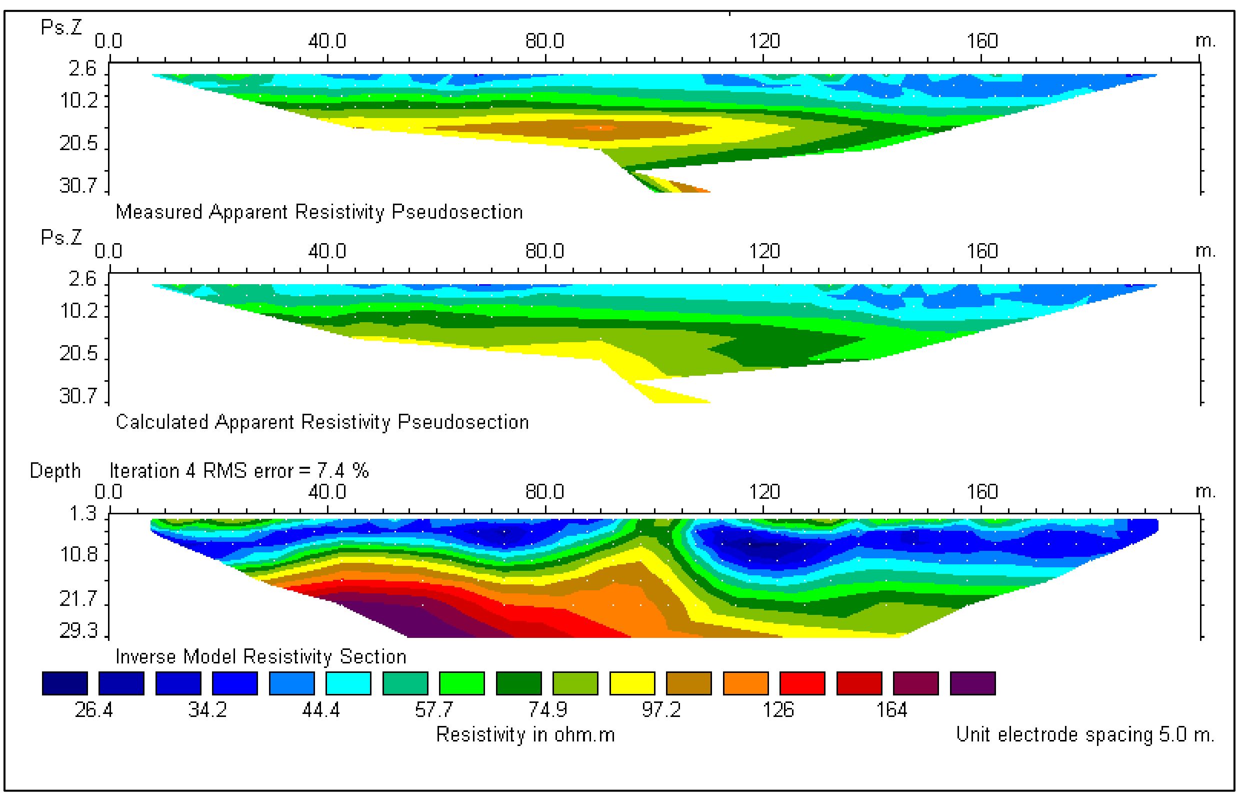

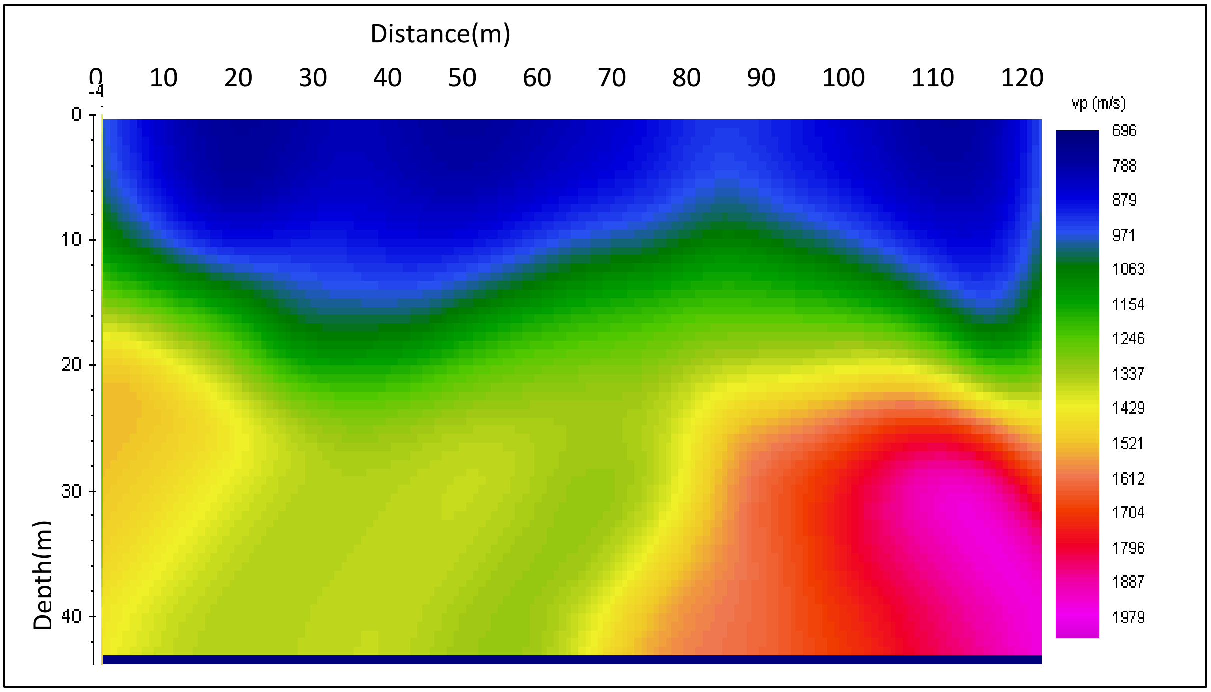

Figure 4: Geoelectric and seismic tomography models for profile 1

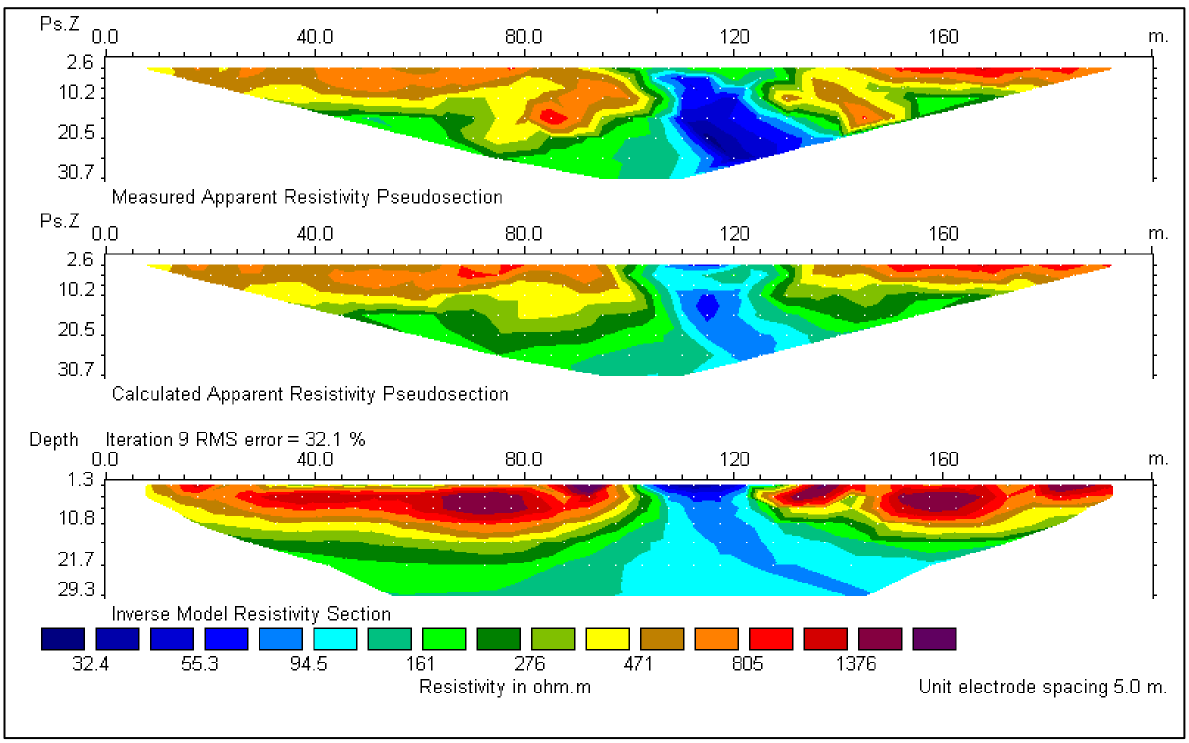

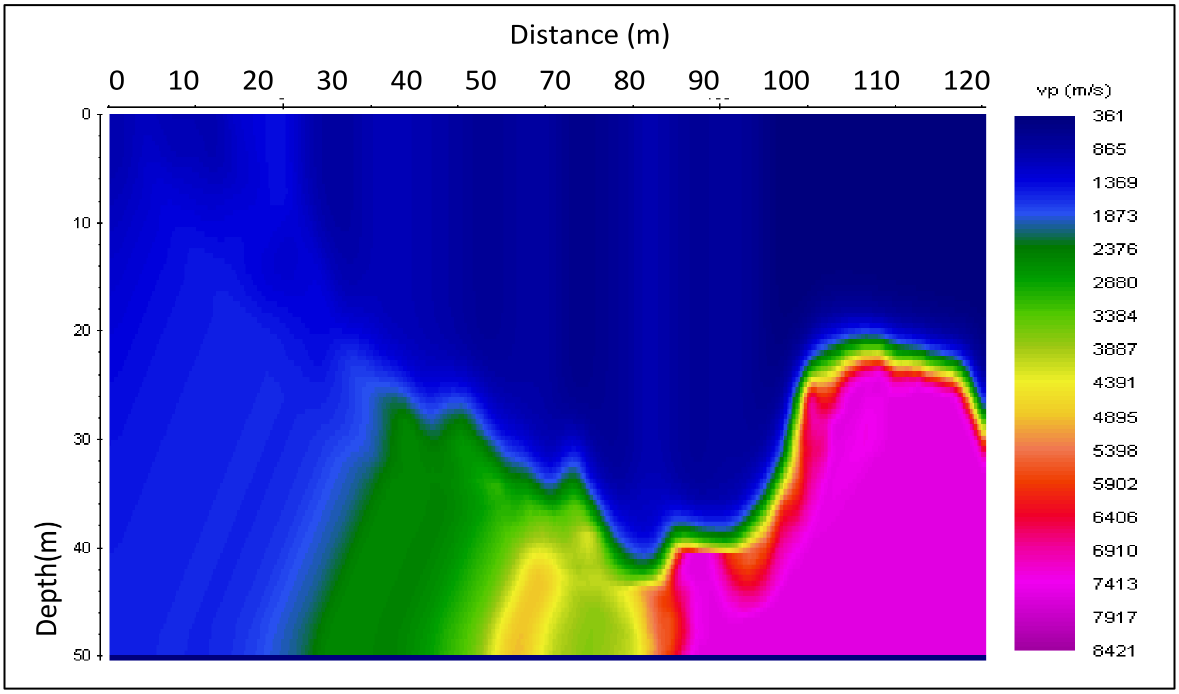

Figure 5: Geo-electric and seismic tomography models for profile 2

CONCLUSION

At the same spread length, seismic refraction tomography clearly probes deeper than geo-electric tomography. It is evident from the geo-electric section's extremely low resistivity that the basement was not probed. On the other hand, seismic refraction tomography revealed multiple signs of high velocities in the region, demonstrating its ability to probe deeper than 40 meters into the underlying topography. Seismic refraction tomography is advised to be used in regions with significant spread length constraints in order to increase the energy source and probe a specific depth of interest.

REFERENCES

Alan, E., Mussett, M., & Aftab, K. (2000). Looking into the earth.

Gregory, S. B. (2002). Near-Surface Seismic Refraction Tomography Tutorial.

Loke, M. H. (2000). Electrical imaging surveys for environmental and engineering studies, a practical guide to 2D and 3D surveys.

Lowrie, W. (1976). Fundamental of Geophyscis, Cambridge University Press.

McCurry, P., (1970). The geology of Degree Sheet 21, Zaria. Unpublished M.Sc. Thesis, Department of Geology, Ahmadu Bello University, Zaria.

Ologe, O., Bankole, S. A., & Adeoye, T. O. (2014). Geo-Electric Study for Groundwater Development in Ikunri Estate, Kogi West, Southwestern Nigeria. *Ilorin Journal of Science*, *1*(1), 154-166.

Osemeikhian J. E. A. and Asokhia. R. (1994). Applied Geophysics, Stamatas Services Ltd.

Oyewoye, M. O., (1964). Geology of the Nigerian Basement Complex, *Journal of Nigerian Mining,* Geological and Metallurgical Society, Vol. 1, pp. 87-102.

Wright, J. B. & McCurry, P. (1970). The geology of Nigeria Sheet 102 SW of Zaria and its region. Edited by M. J. Mortimore. Department of Geography, Ahmadu Bello University, Zaria. Occasional paper, No. 4, pp 2-6.